Talanta 79 (2009) 1433–1440

Contents lists available at ScienceDirect

Talanta

journal homepage: www.elsevier.com/locate/talanta

Ultra-performance liquid chromatographic–electrospray mass spectrometric determination (UPLC-ESI-MS) of *O*-demethylated metabolite of paeonol *in vitro*: Assay development, human liver microsome activities and species differences

Hui-Xin Liu[a,b], Ying Hu[a], Yu-Qi He[c], Yong Liu[a], Wei Li[a,b], Ling Yang[a,*]

[a] *Laboratory of Pharmaceutical Resource Discovery, Dalian Institute of Chemical Physics, Chinese Academy of Sciences, Dalian, China*
[b] *Graduate University of the Chinese Academy of Sciences, Beijing, China*
[c] *Shanghai University of Traditional Chinese Medicine, Shanghai, China*

ARTICLE INFO

Article history:
Received 4 March 2009
Received in revised form 3 June 2009
Accepted 3 June 2009
Available online 13 June 2009

Keywords:
Ultra-performance liquid chromatography
Paeonol
Human liver microsomes
O-Demethylation
Enzyme kinetics
Species differences

ABSTRACT

A simple and sensitive method for determination of the *O*-demethylation activity of rat, dog, minipig, and human liver micrsomes toward paeonol using ultra-performance liquid chromatography with mass detection (UPLC-MS) has been developed. The method uses chemically synthesized *O*-demethylated metabolite of paeonol (2,4-dihydroxyacetophenone, DHA) as a standard for method validation. Validation was done with respect to specificity, linearity, detection limit, recovery, stability, precision and accuracy. The chromatographic separation was achieved on a UPLC BEH C_{18} column (50 mm × 2.1 mm i.d., 1.7 μm), with phase of acetonitrile–water (ratio 30:70). Selective ion reaction (SIR) monitor was specific for paeonol, DHA and I.S. The method was specific since there were no interference peaks from the reaction matrix. The calibration curve for DHA was linear from 0.5–100 μM with r^2 = 0.9999. The newly developed method has good precision and accuracy. The method was successfully used to determine the kinetics of DHA activities toward paeonol in liver microsomes from different species. Dog liver microsomes (DLMs) were the most active in paeonol *O*-demethylation (709.7 pmol/min/mg protein) followed by rat liver microsomes (RLMs) (579.6 pmol/min/mg protein), HLMs (569.3 pmol/min/mg protein), and then minipig liver microsomes (PLMs) (417.3 pmol/min/mg protein). The developed method was appropriated for rapid screening paeonol *O*-demethylation activity in liver microsomes from different species.

1. Introduction

Drug metabolic profile plays an important role in discovering and developing the novel drug from the metabolites possessed the pharmacological activities [1,2]. An understanding of the enzymology of the metabolic clearance of a drug, whether by Phase I or Phase II mechanisms, is pivotal to new drug development [3–6]. Early knowledge of the potential biotransformations of drug in the target species is of great interest [7,8]. Traditionally, rodents such as the rat and nonprimate species such as the dog have been used as animal models in studies aimed at evaluating the pharmacodynamics, metabolism, pharmacokinetics, and safety of new chemical entities [9–12]. The identification of metabolite and metabolic enzymes involved in drug metabolism are important for us to understand which one, parent drug or metabolite(s), is really active and how variations in drug concentrations can lead to differences in drug efficacy and toxicity [13,14]. In addition, knowledge of species differences in drug metabolism will help us to select appropriate animal models to study the drug in question [15,16].

Paeonol (2′-hydroxy-4′-methoxyacetophenone, Fig. 1) is the main active compound of *Moutan Cortex*, the root cortex of *Paeonia suffruticosa* Andrews (family Paeoniaceae), which has antioxidant and anti-inflammatory activity and found to suppress tumor formation [17,18]. As compared to the extensive research of the pharmacological activities of paeonol, few studies have dealt with its metabolism and pharmacokinetics. 2,4-Dihydroxyacetophenone (the only Phase I metabolite of paeonol, DHA) was first detected in plasma of rats treated with purified paeonol alone, in a relatively abundant amount, compared with that of paeonol. In addition, DHA-2-*O*-sulfate (DHAS) was the major Phase II metabolite of paeonol detected in plasma of rats, although several Phase II metabolites were also detected after oral administration of paeonol [19]. It should be pointed out that Phase I reactions usually precedes Phase II reactions [20]. Therefore, paeonol might be demethylated to DHA in the first place, and then sulfated to DHAS. For this reason, paeonol Phase I metabolism could be critical for the clearance

* Corresponding author at: Laboratory of Pharmaceutical Resource Discovery, Dalian Institute of Chemical Physics, Chinese Academy of Sciences, 457, Zhong-shan Road, Dalian 116023, China. Tel.: +86 411 84379317; fax: +86 411 84676961.
E-mail address: yling@dicp.ac.cn (L. Yang).

0039-9140/$ – see front matter © 2009 Elsevier B.V. All rights reserved.
doi:10.1016/j.talanta.2009.06.018

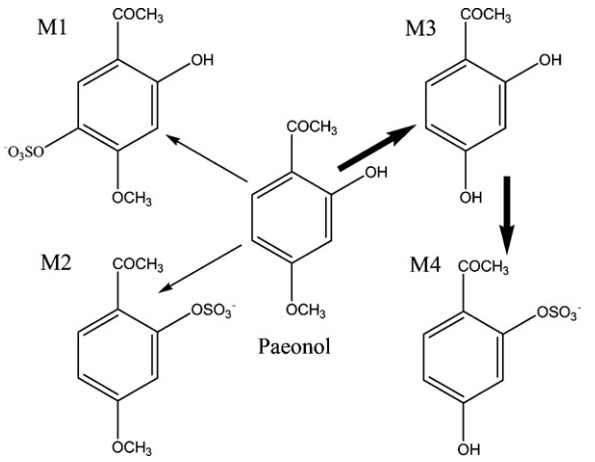

Fig. 1. Proposed metabolic pathway of paeonol. 2-Hydroxy-4-methoxyacetophenone-5-*O*-sulfate (M1), paeonol-2-*O*-sulfate (M2), DHA (M3), and DHA-2-*O*-sulfate (M4).

of paeonol in human. The Phase I metabolism, mainly catalyzed by cytochromes P450 (CYP), plays an important role in the metabolism of many drugs [21,22]. However, no information about the species differences in Phase I metabolism of paeonol is known.

Recently, UPLC was introduced as commercially available instrument, which has been applied for the pharmaceutical, toxicological and biochemical analysis [23–27]. It has the advantages of the fast analysis, high peak capacity, good sensitivity and low consumption of samples [28]. Furthermore, MS techniques play an important role in the metabolism study, because the high sensitivity of MS as an LC detector facilitates the detection of metabolites which are difficult to obtain by conventional means.

The aim of the present study was to find if the species differences occur in paeonol *O*-demethylation in human and animal tissues. For this goal, a rapid and sensitive UPLC-MS method is established for the *in vitro* measurement of paeonol *O*-demethylation in human and animal tissues. Mass and nuclear magnetic resonance (NMR) spectroscopy analyzes were used to establish unequivocally the structure of the demethylated metabolite formed in these reactions. Application of this method was demonstrated by determining enzyme kinetics using human liver microsomes. The method was also employed to characterize the kinetics of paeonol *O*-demethylation in RLMs, PLMs, and DLMs for which no data are currently available. And then, interspecies differences in enzyme activities were evaluated in four species.

2. Experimental

2.1. Reagent and chemicals

Paeonol (purity ≥99%), D-glucose-6-phosphate (G-6-P), glucose-6-phosphate dehydrogenase (G-6-PDH), and $NADP^+$ were purchased from Sigma–Aldrich (St. Louis, MO, USA). All other materials were of the highest quality commercially available.

Source of HLMs has been previously reported [29,30]. In brief, human livers were obtained from autopsy samples (n = 9, male Chinese, ages from 27 to 48) from Dalian Medical University, with the approval of the ethics committee of Dalian Medical University. The medication history of the donors was not known. The relative activities of individual cytochrome P450 enzymes among the individual microsomal preparations had been determined previously using specific cytochrome P450 substrates, and the results showed similar metabolic rates compared to health samples [31,32]. Research involving human subjects was done under full compliance with government policies and the Helsinki Declaration. Liver specimens were stored in liquid nitrogen until preparation of microsomes.

Procedures involving animals complied with the Laboratory Animal Management Principles of China. Sprague–Dawley (SD) rats (n = 10, male, weight 180–220 g) were purchased from Dalian Medical University. The animals had free access to tap water and pellet diet. All the rats were euthanized by decapitation, and livers were rapidly excised and pooled for preparation of microsomes.

Colony-bred Chinese Bama minipigs weighing 10–12 kg (n = 6, male, age 6 months) and beagle dogs weighing 10–12 kg (n = 3, male, age 12 months) were obtained from Department of Animal Science, Third Military Medical University, China. The animals were euthanized by i.v. injection of pentobarbital sodium (150 mg/kg b.wt.); tissue samples were taken from the left medial lobe of the liver within 5 min after death. Liver samples were pooled together to prepare microsomes.

Microsomes were prepared from liver tissue by differential ultracentrifugation. Protein concentrations of the microsomal fractions were determined by the Lowry method using bovine serum albumin as a standard [33]. Determination of CYPs content was performed according to Omura and Sato [34].

2.2. Microsomal incubations.

The incubation mixture, with a total volume of 200 μL, included 100 mM potassium phosphate buffer, pH 7.4, NADPH-generating system (1 mM $NADP^+$, 10 mM glucose 6-phosphate, 1 unit/ml glucose-6-phosphate dehydrogenase, and 4 mM $MgCl_2$), liver microsomes (0.3 mg/mL), and paeonol (10 μM). After preincubation of the medium at 37 °C for 3 min, the reaction started with the addition of Paeonol. Paeonol was previously dissolved in methanol, with a final methanol concentration below 1% (v/v) in the reaction mixture. The reactions were terminated by the addition of methanol (100 μL), followed by centrifugation at 20,000 × g for 10 min at 4 °C to obtain the supernatant. Aliquots of supernatants 10 μL were then analyzed by UPLC with MS detector. Control incubations without NADPH or without substrate or without microsomes were carried out to ensure that metabolites formation were microsomes and NADPH dependent.

1-Aminobenzotriazole (ABT, a broad CYPs inhibitor [35]), was used tentatively to identify the metabolite peak as CYP-catalyzed *O*-demethylation. ABT (50 μM) was respectively preincubated with liver microsomes from different species and NADPH-generation system for 20 min, and then the reaction was initiated by adding paeonol. Paeonol and the inhibitors were previously dissolved in methanol, with a final methanol concentration below 1% (v/v) in the reaction mixture. The same concentration of methanol was added in the control incubation. The reaction products were analyzed by UPLC with MS detector as described above.

2.3. UPLC-MS conditions.

All analyzes were performed on Waters Acquity UPLC system (Waters, MA, USA), including binary solvent manager, autosampler manager, column compartment, single quadrupole mass spectrometry, connected with Waters MassLynx V4.1 software. An Acquity UPLC BEH C_{18} column (50 mm × 2.1 mm i.d., 1.7 μm) was used. The column temperature was maintained at 45 °C. The isocratic mobile phase composition was a mixture of water–acetonitrile (70:30, v/v). The flow rate was set at 0.3 mL/min and the injection volume was 10 μL. Negative ion of $[M-H]^-$ of DHA which was 151 and $[M-H]^-$ of I.S. which was 137 were used for determination with the SIR mode. The full-scan mass spectra are shown in Fig. 2. In order to optimize the MS parameters, a standard solution (10 μM) of DHA was infused into the mass spectrometer. For DHA, the following optimized parameters were obtained: capillary voltage: 3.2 kV, cone

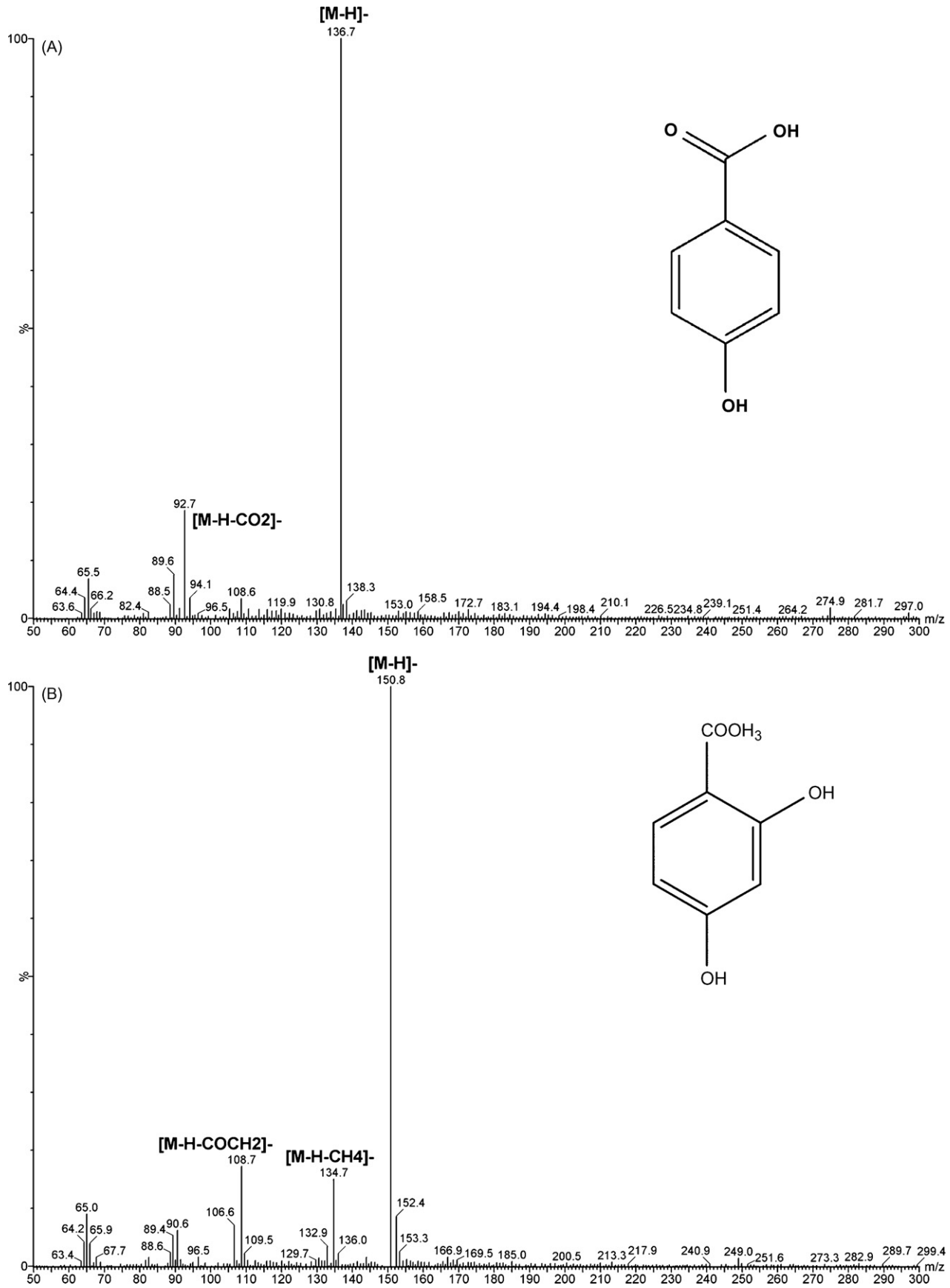

Fig. 2. Negative ion spectra of $[M-H]^-$ of I.S. (A) and $[M-H]^-$ of DHA.

voltage: 40 V, extractor voltage: 1 V, RF lens: 0.5 V, source temp: 100 °C, desolvation temp: 350 °C, desolvation gas flow: 550 (L/h), cone gas flow: 50 (L/h).

2.4. Metabolite purification.

To facilitate further metabolite identification and allow calibration, a small amount (approximately 5 mg) of DHA was biologically synthesized and purified as follows. The incubation system was scaled up to 250 mL. Paeonol (50 μM) was respectively incubated with liver microsomes from different species (1.0 mg/mL) and NADPH-generating system (1 mM $NADP^+$, 10 mM glucose-6-phosphate, 1 unit/mL of glucose-6-phosphate dehydrogenase, and 4 mM $MgCl_2$) for 90 min at 37 °C. Under these conditions, about 20% of paeonol was converted to DHA. The reaction mixture was extracted with 50% ethyl acetate, and the organic layer was separated after the reaction mixture was centrifuged at 9000 × *g* for 10 min. The extraction procedure was repeated three times and the organic layer was combined. The organic phase was dried in vacuo, and the residue was dissolved in methanol (1.5 mL) and 50 μL of the solution was injected into the HPLC. The HPLC system (SHIMADZU, Kyoto, Japan) consisted of a SCL–10A system controller, two LC–10AT pumps, a SIL–10A auto injector, a SPD–10AVP UV detector and a Shim-pack (Shimadzu corporation) C_{18} column (4.6 mm × 150 mm, 5 μ) was used to separate paeonol and its metabolite. The mobile phase was 65% methanol in water. The eluent was monitored at 274 nm with a flow rate of 1.0 mL/min, and the eluent containing the metabolite was collected and dried in vacuo. The purity of metabolite was about 98% (HPLC).

2.5. ^{1}H-NMR spectroscopy

^{1}H-NMR spectroscopy was used to confirm the structural identity of the HPLC-purified metabolite peaks, respectively. Proton NMR spectra was obtained at 400 MHz on a Bruker AV-400 spectrometer (Bruker, Newark, Germany). Compounds were dissolved in DMSO-d_6 and experiments were conducted at 21 °C. Chemical shifts are reported in ppm with reference to tetramethylsilane.

2.6. Standards

Stock solution at a concentration of 10 mM in methanol was prepared for DHA. Different concentrations of DHA solutions (50–1000 μM) were prepared by serial dilutions of 10 mM stock solution with methanol. 2 μL of each DHA solution was respectively used to mix with 20 μL liver microsomes, 20 μL glucose-6-phosphate, 20 μL glucose-6-phosphate dehydrogenase, 10 μL $NADP^+$ and 20 μL $MgCl_2$, and different volumes of 100 mM potassium phosphate buffer was added to make the system volume to be 200 μL, and made the concentration of DHA 0.5–100 μM in 200 μL system, then 100 μL stop solution containing internal standard (4-hydroxybenzoic acid, 30 μM) was added. After centrifugation, these standard solutions were used to prepare the calibration curves and quality control (QC) samples. The calibration curves were obtained daily for 6 days using nine different amounts of DHA (0.5, 1, 2, 5, 10, 25, 50, 75, and 100 μM); curves were demonstrated by the statistical analysis of linear regression model of $y = ax + b$ (where x represents concentration of DHA and y represents the peak area ratio of DHA to I.S.); calibration curve data points represent the mean of sextuplicate determinations. These standard solutions were stored at −20 °C and were stable for at least 4 weeks. Working solutions were freshly prepared each day and were obtained by dilution from the stock solutions as stated above.

2.7. Method validation

The specificity of the method was assessed to evaluate the influence of the matrix and non-enzymatic reactions in blank samples.

The QC samples (0.5, 30, and 80 μM) were analyzed with the calibration standards (0.5–100 μM). The lower limit of detection (LLOD) for DHA was defined as the quantity of DHA corresponding to three times the baseline noise (signal-to-noise ratio of 3). LLOD was assessed using the 0.5 μM standard solutions. The lower limit of quantitation (LLOQ) of the assay, defined as the lowest concentration on the calibration curve that can be quantitated with accuracy within 15% of nominal and precision not exceeding 20% [36,37]. The recovery of DHA was estimated by comparing the peak area of the extracted DHA to that of the analyte diluted stock solutions at three different concentrations level (0.5, 30, and 80 μM) using six replicates at each level [38]. The calibration curve had to have a correlation coefficient (r) of 0.99 or better. The acceptance criterion for each back-calculated standard concentration was <15% deviation from the nominal value except at LLOQ, which was set at <20% [36,37].

The intra-day accuracy and precision were determined at three different levels of concentration from six replicate QC samples. The inter-day accuracy and precision were determined at three levels of concentrations from six replicate QC samples on three independent occasions. The precision was calculated as the relative standard deviation (RSD) of the mean with RSD (%) = (standard deviation of the mean/mean) × 100, while the accuracy was calculated as relative mean error (RME) with RME (%) = [(mean − theoretical concentration)/theoretical concentration] × 100. The acceptable intra- and inter-precision (RSD) and accuracy (RME) were set at <15% [39].

To check the stability of the biological matrix, liver microsomes were spiked with DHA at three concentrations (0.5, 30, and 80 μM). The stability was assessed after storage in a refrigerator (4 °C) and at room temperature (25 °C) for various intervals (8, 24, and 72 h), by comparing peak areas from initial and subsequent determinations. The precision was assessed by mean ± SD%, while the accuracy was calculated as RME.

2.8. Kinetic analysis

Incubation conditions were chosen such that product formation was linear with respect to both microsomal protein amount and incubation time for the determination of *O*-demethylation activities toward paeonol in HLMs, PLMs, RLMs, and DLMs, respectively. The microsomal protein amounts and incubation time for the determination of *O*-demethylation activities were 30 μg and 30 min, respectively. Substrate concentrations for the determination of *O*-demethylation activities were from 2.5 to 200 μM. The Michaelis–Menten parameters, such as K_m and V_{max}, were estimated by analyzing Eadie–Hofstee plots.

2.9. Statistics

Potential differences in paeonol *O*-demethylation activities related to species were evaluated by the two-tailed Student's-*t* test with a $p < 0.05$ indicating a significant difference [7]. All activities were determined in duplicate and averaged.

3. Results

3.1. Identification of paeonol metabolite

After paeonol was respectively incubated with liver microsomes from different species and NADPH-generating system, one new peak was eluted at 2.6 min (Fig. 3). The new peak was not

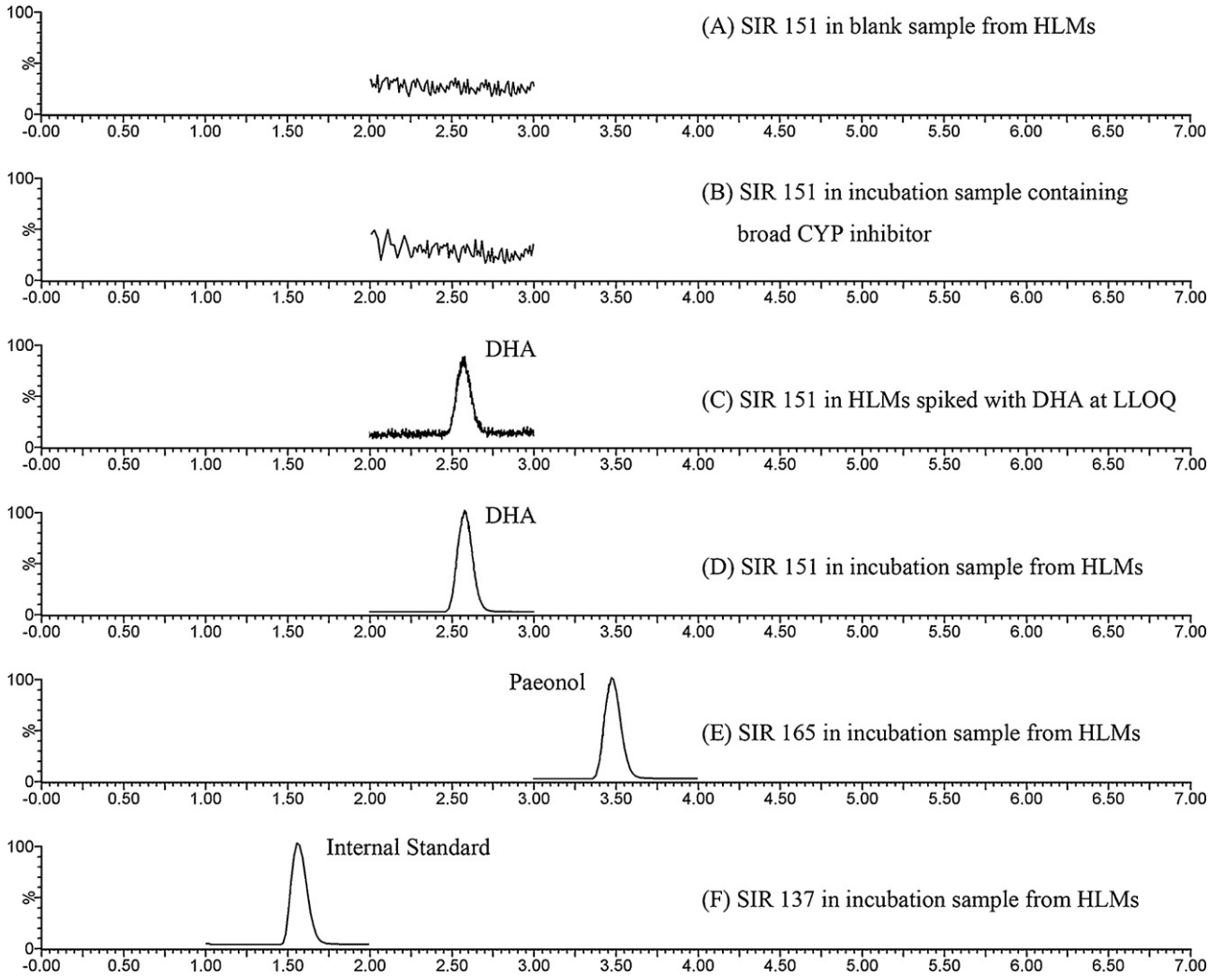

Fig. 3. UPLC analysis of *O*-demethylation activity toward paeonol in HLMs.

observed in the negative controls without NADPH, or without substrate, or without microsomes, or incubation samples containing broad CYP inhibitor (1-aminobenzotriazole) (Fig. 3). The ESI mass spectra of the peaks showed a deprotonated molecule at *m*/*z* 151 ($[M-H]^-$), respectively, indicating the molecular weight of the metabolite as 152, corresponding to the demethylated metabolite of paeonol (Fig. 2). The ^{1}HNMR spectra of paeonol and its metabolite indicated that the $-COCH_3$ group was intact, however, the most distinct spectra change was involved in the $-OCH_3$ group (Table 1). These observations suggested that the demethylation type was *O*-demethylation not *C*-demethylation. In combination, the metabolite of paeonol in different liver microsomes incubation systems were respectively identified as *O*-demethylated metabolite, 2,4-dihydroxyacetophenone.

Table 1
^{1}HNMR data for paeonol and its metabolite (DHA).

Paeonol	DHA	Position
2.52 (3H, s)	2.52 (3H, s)	$-COCH_3$
3.82 (3H, s)	–	$-OCH_3$
6.47 (1H, d, *J* = 2.5 Hz)	6.47 (1H, d, *J* = 2.5 Hz)	H-3
6.53 (1H, dd, *J* = 8.9, 2.5 Hz)	6.38 (1H, dd, *J* = 8.9, 2.3 Hz)	H-5
7.85 (1H, d, *J* = 8.9 Hz)	7.76 (1H, d, *J* = 8.9 Hz)	H-6
12.64 (1H, s)	12.61 (1H, s)	H-2

3.2. Method validation

Under the UPLC-MS conditions described above, peaks were adequately separated. The specificity of the method was assessed to evaluate the influence of the matrix from liver microsomes and non-enzymatic reactions. The interfering peaks for the determination of DHA were not detected in blank samples (Fig. 3).

Calibration curves exhibited good linearity in the range of 0.5–100 μM, with coefficients of correlation (r^2) 0.9999 for DHA. The intra- and inter-day precision, expressed as RSD, and accuracy expressed as RME are reported in Table 2. Recoveries from liver microsomes spiked with DHA at concentrations of 0.5, 30 and 80 μM were 98.7%, 99.3%, and 101.2%, respectively. LLOD determined experimentally was 0.05 μM for DHA.

3.3. Stability and reproducibility studies

DHA was stable for 72 h at 4 °C and at 25 °C in liver microsomes (Table 3). The percentage recoveries were similar at all concentrations. The reproducibility of the assay was determined by analysis of paeonol *O*-demethylation activities in HLMs. Three concentrations (5, 50, and 150 μM) were chosen. The results are summarized in Table 4. Intra- and inter-day reproducibilities (expressed as RSD) were better than 4.6% at all substrate concentrations.

Table 2
Precision and accuracy of DHA calibration standards and QC samples ($n = 6$).

Nominal concentration (μM)	Mean calculated concentration (μM)	Accuracy (RME%)	Precision (RSD%)
Intra-day			
Calibration standards			
0.50	0.47	−6.00	3.47
1.00	0.98	−2.27	1.41
2.00	1.96	−1.75	1.59
5.00	4.94	−1.12	1.45
10.00	9.92	−0.79	2.47
25.00	25.54	2.18	4.19
50.00	49.92	−0.16	1.15
75.00	74.20	−1.06	2.28
100.00	100.41	0.41	1.64
Quality control samples			
0.50	0.48	−3.81	3.94
30.00	29.99	−0.03	1.08
80.00	80.89	1.12	1.05
Inter-day			
Calibration standards			
0.50	0.47	−5.49	5.03
1.00	0.98	−1.66	2.04
2.00	2.05	2.97	6.25
5.00	5.16	3.33	4.64
10.00	10.22	2.18	2.35
25.00	25.59	2.36	3.97
50.00	50.41	0.82	2.41
75.00	77.95	3.94	1.53
100.00	102.34	2.34	1.30
Quality control samples			
0.50	0.48	−4.66	2.79
30.00	30.37	1.22	1.64
80.00	81.84	2.30	3.10

Table 3
Stability data of DHA in spiked liver microsomes under various conditions ($n = 3$).

Storage conditions		0.5 μM		30 μM		80 μM	
		(mean ± SD %)	RME (%)	(mean ± SD %)	RME (%)	(mean ± SD %)	RME (%)
4 °C	8 h	96.75 ± 1.30	−3.24	103.39 ± 0.95	3.38	103.79 ± 2.26	3.79
	24 h	96.26 ± 2.46	−3.73	97.76 ± 3.67	−2.23	101.09 ± 1.78	1.09
	72 h	95.67 ± 3.56	−4.32	101.22 ± 5.31	1.22	102.83 ± 1.32	2.83
25 °C	8 h	95.77 ± 3.26	−4.23	100.89 ± 4.06	0.89	102.30 ± 3.10	2.30
	24 h	96.63 ± 2.18	−3.36	101.76 ± 3.22	1.76	102.01 ± 3.44	2.01
	72 h	95.66 ± 3.45	−4.33	104.07 ± 2.24	4.07	104.07 ± 2.23	4.07

3.4. Optimization of reaction condition

For these studies, substrate concentration of 20 μM for paeonol was used. The paeonol *O*-demethylation formation was linear for at least 60 min in liver microsomes from different species ($r^2 = 0.997$). Similarly, in assays of CYP activities toward paeonol in liver microsomes from different species, the formation of paeonol *O*-demethylation was found to be linear up to 125 μg of microsomal protein ($r^2 = 0.999$).

Table 4
Intra- and inter-day duplicability of the assay for paeonol *O*-demethylation activities toward DHA in HLMs[a] ($n = 6$).

Substrate concentration (μM)	Activity (mean ± SD%) (nmol/min/mg protein)	RSD (%)
Intra-day		
5.00	235.23 ± 7.84	3.33
50.00	564.22 ± 11.14	4.52
150.00	678.90 ± 14.10	3.53
Inter-day		
5.00	230.91 ± 7.08	3.06
50.00	567.31 ± 12.08	4.26
150.00	677.23 ± 11.22	2.83

[a] Reactions were performed in the presence of paeonol (5, 50, and 150 μM) and human liver microsomal protein (30 μg) in a total volume of 200 μL for 30 min at 37 °C. The method of sample preparation and the UPLC-MS conditions are described in Section 2.

3.5. Enzyme kinetics and species differences

This enzyme kinetics study of paeonol *O*-demethylation in HLMs showed that K_m was 16.8 ± 4.1 μM and V_{max} was 569.3 ± 10.9 nmol/min/mg of protein (mean ± SD%). The substrate concentration-*O*-demethylation velocity curves followed typical Michaelis–Menten kinetics, and the Eadie–Hofstee plot for paeonol *O*-demethylation was monophasic (Fig. 4). The enzyme kinetics study of paeonol *O*-demethylation in liver microsomes from different species was shown in Table 5. As shown in Fig. 5, paeonol *O*-demethylation activities in liver microsomes at 15 μM paeonol concentration varied between species with 204.1 pmol/min/mg protein in rat livers to as high as 373.2 pmol/min/mg protein in dog livers. Dog was found to have significantly higher paeonol *O*-demethylation activity than rat (1.8-fold) and minipig (1.6-fold), while no significant differences were observed between human, rat, and minipig.

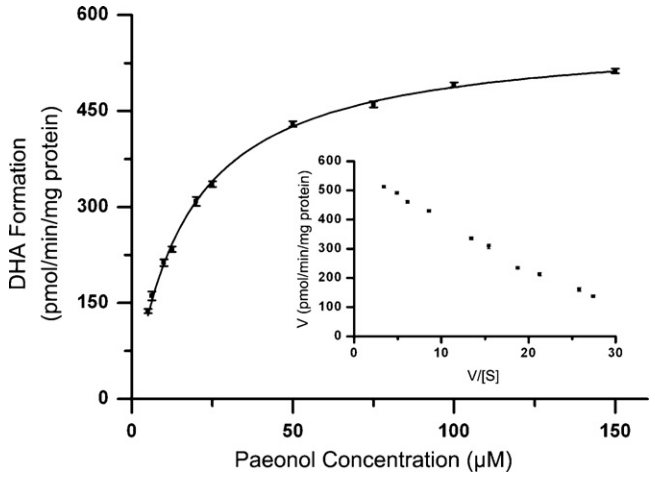

Fig. 4. Enzyme kinetics of DHA in human liver microsomes. The Eadie–Hofstee plot is shown as an inset. Each point represents the mean of three separate experiments performed in duplicate.

Table 5
Kinetic parameters of paeonol metabolism in liver microsomes from different species[a] ($n = 3$).

Species	K_m (μM)	V_{max} (nmol/min/mg protein)
Human	16.8 ± 4.1	569.3 ± 10.9
MiniPig	9.5 ± 1.4	417.3 ± 8.9
Rat	24.7 ± 5.2	579.6 ± 12.6
Dog	13.1 ± 3.2	709.7 ± 12.1

[a] Reactions were performed in the presence of paeonol (2.5–200 μM) and liver microsomal protein (30 μg) in a total volume of 200 μL for 30 min at 37 °C. The method of sample preparation and the UPLC-MS conditions are described in Section 2.

4. Discussion

O-Demethylation plays an important role in the clearance of paeonol. However, no information about the species differences in paeonol *O*-demethylation is known. For this reason, we first developed a rapid and specific UPLC-MS method for the qualitative and quantitative determination of paeonol *O*-demethylation activity in human and animal tissues. Application of this method was then demonstrated by determining enzyme kinetics using liver microsomes from different species and the kinetic parameters obtained from different species by this method were compared with each other.

We detected one metabolite of paeonol in human and animal tissues by first investigating paeonol *O*-demethylation reaction in liver microsomes from different species. Positive identification of the metabolite peak as mainly CYP-catalyzed metabolism was based on a requirement for $NADP^+$ in liver microsomes incubation system, and ABT (a nonspecific inhibitor of CYPs) showed potent inhibitory effects against the produce (Fig. 3). The ESI mass spectra of the peak typically formed after incubation of paeonol with $NADP^+$ in liver microsomes showed a deprotonated molecule at m/z 151 ($[M-H]^-$), indicating the molecular weight of the metabolite as 152, corresponding to the demethylated metabolite of paeonol. Since there are two possible mechanism of demethylation on paeonol, including *O*-demethylation and *C*-demethylation, NMR was used to determine the structure of the metabolite. In this case, the most important thing is the chemical shift of the methyl group. The methyl group linked to a carbonyl carbon atom was remained according to the ^{1}HNMR spectra of paeonol and its metabolite (Table 1). Therefore, the peak was identified as the *O*-demethylated metabolite of paeonol, 2,4-dihydroxyacetophenone.

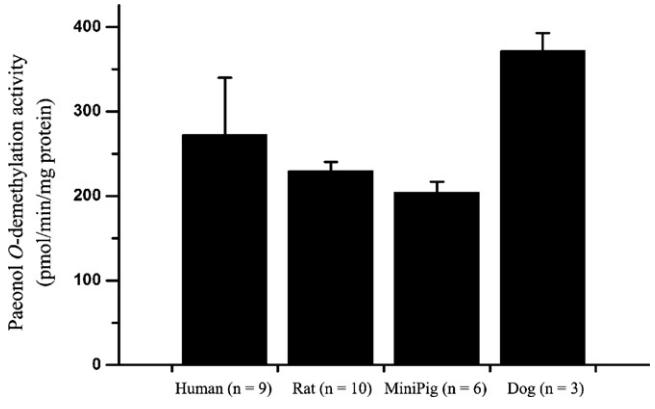

Fig. 5. Species comparative paeonol *O*-demethylation by liver microsomes. Bars are mean activity values, while the error bars indicate the standard error of estimate.

UPLC has the advantages of the fast analysis, high peak capacity, high sensitivity and low consumption of samples compared with HPLC, which makes it more suitable for the pharmaceutical, toxicological and biochemical analysis studies [23,28]. With the great resolution and expeditiousness, UPLC was used here for separation. To clean the incubation sample, a step of high-speed centrifugation was adopted, and the time of sample preparation needed was finished within 1 h. Higher column temperature was used so as to decrease the pressure at higher flow rate, which could improve the separation and peak shape. To elevate the reproducibility of separation and simplify the experiment, a simple elution system was selected, and the run time was less than 3 min. The preparation and separation of per sample using this UPLC-MS method was simple and rapid with a higher sensitivity, which may prove to be useful in measuring paeonol *O*-demethylation activities in animal and human tissues with very low levels of this enzyme.

It is necessary to use an I.S. to obtain good accuracy and precision when a mass spectrometer is used as the LC detector. 4-Hydroxybenzoic acid was adopted as I.S. because of the similarity of its retention to metabolite and good ionization characteristics under the MS conditions. The ESI in negative ion mode was adopted for the MS determination of the metabolite. The SIR mode was selected. The test results showed that the base peak in the mass spectra of the metabolite was at m/z 151, which was the ion $[M-H]^-$ of the metabolite. The intensity of the $[M-H]^-$ was stable and reproducible. Therefore, it was selected as the target ion for metabolite. In the same condition, the base peak in the mass spectrum of the I.S. was at m/z 137, which was the protonated molecule $[M-H]^-$ of the I.S. Therefore, the ion at m/z 137 was selected as the target ion for the I.S. Under the optimized UPLC-MS conditions, no interfering peaks were detected for the DHA or I.S. in blank samples from HLMs (Fig. 3).

The coefficients of variations of slope for DHA were found to be <15%, which indicate a high precision of the present assay (Table 2). Intra- and inter-day precision was <6.3% for all concentrations of DHA in HLMs. It was demonstrated that the UPLC-MS method for the determination of DHA was reliable and reproducible since both precision and accuracy were below 10% for all estimated concentrations of DHA (Table 2). Usually, the samples for *in vitro* kinetic study using liver microsomes should be analyzed as soon as possible or within short-term storage. Thus, we assessed samples at three concentrations after storage in a refrigerator (4 °C) and at room temperature (25 °C) for various intervals (8, 24, and 72 h), which could reflect situations likely to be encountered during actual sample handling and analysis. The results showed in Table 3 suggested that HLMs containing the metabolite can be handled under normal laboratory conditions without significant loss of compound.

The UPLC-MS method developed was successfully used to the determination of paeonol *O*-demethylation activities, such as

kinetic studies with excellent precision and accuracy (Table 4). With the method described here, the kinetics in liver microsomes from different species were rapidly and precisely determined (Table 5). The K_m value obtained from DLMs was close to that of HLMs (13.1 *versus* 16.8), and the V_{max} value obtained from RLMs was close to that of HLMs (579.6 *versus* 569.3). In general, no one species was more active in metabolizing paeonol even though it was interesting to note that dog had significantly greater activities than the two other target animals. More variability is seen in the human metabolic activity than any other species. This was expected as the humans in this study were taken from the general population, while the other species were from inbred laboratory strains. The laboratory animals have therefore many fewer genetic differences. Also their environments and diet are the same, eliminating possible factors that could contribute to differential induction of some of the CYPs [7]. If this study had been conducted using dogs, rats, and pigs obtained from the general population, more variability in the metabolic data would have been expected. Though, there was no metabolic profile difference among paeonol *O*-demethylation in different species, paeonol metabolism in different species needs to be further studied.

5. Conclusion

A UPLC method was developed for the first time for separation of paeonol and its metabolite in human and animal tissues. ESI-MS was used to confirm structure of the demethylated metabolite of paeonol, and the *O*-demethylated metabolite was proved by NMR. The proposed UPLC-MS method was simple, robust and sensitive, revealing that it was appropriate for rapid screening paeonol *O*-demethylation activity in liver microsomes from different species.

Acknowledgements

This work was supported by the National Key Technology R&D Program in the 11th Five year Plan of China (2008ZX10208), National Basic Research Program of China (2009CB522808), National Science & Technology Pillar Program in the 11th Five year Plan of China (2006BAI11B08 and 2008BAI51B02).

References

[1] C. Prakash, C.L. Shaffer, A. Nedderman, Mass Spectrom. Rev. 26 (2007) 340.
[2] P. Baranczewski, A. Stańczak, K. Sundberg, R. Svensson, A. Wallin, J. Jansson, P. Garberg, H. Postlind, Pharmacol. Rep. 58 (2006) 453.
[3] M.G. Soars, R.J. Riley, K.A. Findlay, M.J. Coffey, B. Burchell, Drug Metab. Dispos. 29 (2001) 121.
[4] N.J. Clarke, D. Rindgen, W.A. Korfmacher, K.A. Cox, Anal. Chem. 73 (2001) 430.
[5] R. Kostiainen, T. Kotiaho, T. Kuuranne, S. Auriola, J. Mass Spectrom. 38 (2003) 357.
[6] R. Laine, Curr. Drug Metab. 9 (2008) 921.
[7] N. Chauret, A. Gauthier, J. Martin, D.A. Nicoll-Griffith, Drug Metab. Dispos. 25 (1997) 1130.
[8] Y. Mano, T. Usui, H. Kamimura, J. Pharm. Sci. 97 (2008) 2805.
[9] M.E. Andersen, K. Krishnan, Environ. Health Perspect. 102 (1994) 103.
[10] M.E. Andersen, Toxicol. Lett. 138 (2003) 9.
[11] L. Liu, K.S. Pang, Eur. J. Pharm. Sci. 29 (2006) 215.
[12] W.A. Chiu, H.A. Barton, R.S. DeWoskin, P. Schlosser, C.M. Thompson, B. Sonawane, J.C. Lipscomb, K. Krishnan, J. Appl. Toxicol. 27 (2007) 218.
[13] R.F. Henderson, Chem. Biol. Interact. 135–136 (2001) 53.
[14] S.S. Singh, Curr. Drug Metab. 7 (2006) 165.
[15] J.L. Nieusma, D.J. Claffey, D.R. Koop, W. Chen, R.M. Peter, S.D. Nelson, J.A. Ruth, D. Ross, Toxicol. Lett. 95 (1998) 123.
[16] J.C. Lipscomb, T.S. Poet, Pharmacol. Ther. 118 (2008) 82.
[17] J.G. Chung, Food Chem. Toxicol. 37 (1999) 327.
[18] T.C. Chou, Br. J. Pharmacol. 139 (2003) 1146.
[19] F.B. Gjertsen, E. Solheim, R.R. Scheline, Xenobiotica 18 (1988) 225.
[20] T. Iyanagi, Int. Rev. Cytol. 260 (2007) 35.
[21] S. Narimatsu, R. Yonemoto, K. Masuda, T. Katsu, M. Asanuma, T. Kamata, M. Katagi, H. Tsuchihashi, T. Kumamoto, T. Ishikawa, S. Naito, S. Yamano, N. Hanioka, Biochem. Pharmacol. 75 (2008) 752.
[22] C. Sauer, F.T. Peters, A.E. Schwaninger, M.R. Meyer, H.H. Maurer, Chem. Res. Toxicol. 21 (2008) 1949.
[23] H.X. Liu, Y.Q. He, Y. Hu, Y. Liu, J.W. Zhang, W. Li, Z.T. Wang, L. Yang, J. Chromatogr. B 870 (2008) 84.
[24] L.G. Apollonio, D.J. Pianca, I.R. Whittall, W.A. Maher, J.M. Kyd, J. Chromatogr. B 836 (2006) 111.
[25] X.J. Li, A. Fekete, M. Englmann, C. Gotz, M. Rothballer, M. Frommberger, K. Buddrus, J. Fekete, C.P. Cai, P. Schroder, A. Hartmann, G. Chena, P. Schmitt-Kopplin, J. Chromatogr. A 1134 (2006) 186.
[26] D. O'Connor, R. Mortishire-Smith, D. Morrison, A. Davies, M. Dominguez, Rapid Commun. Mass Spectrom. 20 (2006) 851.
[27] E.C.Y. Chan, S.L. Yap, A.J. Lau, P.C. Leow, D.F. Toh, H.L. Koh, Rapid Commun. Mass Spectrom. 21 (2007) 519.
[28] L. Novakova, L. Matysova, P. Solich, Talanta 68 (2006) 908.
[29] H.X. Liu, Y. Liu, J.W. Zhang, W. Li, H.T. Liu, L. Yang, Drug Metab. Dispos. 36 (2008) 1562.
[30] J.W. Zhang, Y. Liu, J.Y. Zhao, L.M. Wang, G.B. Ge, Y. Gao, W. Li, H.T. Liu, H.X. Liu, Y.Y. Zhang, J. Sun, L. Yang, Drug Metab. Dispos. 36 (2008) 2292.
[31] W. Li, Y. Liu, Y.Q. He, J.W. Zhang, Y. Gao, G.B. Ge, H.X. Liu, H. Huo, H.T. Liu, L.M. Wang, J. Sun, Q. Wang, L. Yang, Xenobiotica 38 (2008) 1551.
[32] J.W. Zhang, Y. Liu, J. Cheng, W. Li, H. Ma, H.T. Liu, J. Sun, L.M. Wang, Y.Q. He, Y. Wang, Z.T. Wang, L. Yang, J. Pharm. Pharm. Sci. 10 (2007) 496.
[33] O.H. Lowry, N.J. Rosebrough, A.L. Farr, R.J. Randall, J. Biol. Chem. 193 (1951) 265.
[34] T. Omura, R. Sato, J. Biol. Chem. 239 (1964) 2370.
[35] P.R. Ortiz de Montellano, J.M. Mathews, Biochem. J. 195 (1981) 761.
[36] X. Li, C. Yu, Y. Cai, G. Liu, J. Jia, Y. Wang, J. Chromatogr. B 820 (2005) 41.
[37] K. Patel, S.M. Guichard, D.I. Jodrell, J. Chromatogr. B 863 (2008) 19.
[38] S. Pedraglio, M.G. Rozio, P. Misiano, V. Reali, G. Dondio, C. Bigogno, J. Pharm. Biomed. Anal. 44 (2007) 665.
[39] F. He, H.C. Bi, Z.Y. Xie, Z. Zuo, J.K. Li, X. Li, L.Z. Zhao, X. Chen, M. Huang, Rapid Commun. Mass Spectrom. 21 (2007) 635.